THIS MONTH IN JNM

Weber looks at the sometimes-puzzling phenomenon of brown-fat radiotracer uptake and recent innovations that promise to resolve some of the imaging difficulties it has posed for nuclear medicine specialists. . . . . ***Page 1101***

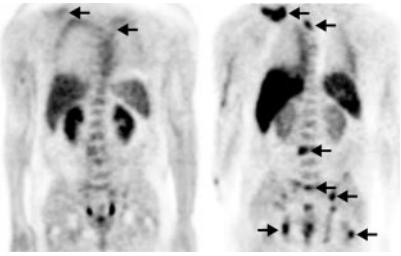

Goldsmith comments on difficulties in establishing the relationship between radiation-absorbed dose and radiobiologic response and advocates the determination of the microdosimetry of tracers on a microscopic and histopathologic scale. . . . . ***Page 1104***

Strauss et al. assess current research on the relationship of ^{18}F-FDG localization to macrophage activity in atherosclerosis and note that this relationship is likely to be a key to predicting significant cardiac events. . . . . ***Page 1106***

Kasama et al. present scintigraphic and other evidence suggesting that atrial natriuretic peptide can benefit cardiac sympathetic nerve activity and improve left ventricular remodeling in patients with acute heart failure. . . . . ***Page 1108***

Kurata et al. report on a study using ^{123}I-MIBG imaging to determine whether kidney transplantation improves cardiac sympathetic nervous system function. . . . . ***Page 1114***

Akashi et al. used ^{123}I-MIBG myocardial scintigraphy to uncover significant clues to the origins of reversible left ventricular dysfunction in patients with "takotsubo" cardiomyopathy. . . . . ***Page 1121***

Slomka et al. introduce a novel "motion-frozen" technique to improve the image quality and accuracy of gated myocardial perfusion SPECT by eliminating the influence of cardiac left ventricular motion on display and quantification. . . . . ***Page 1128***

Whone et al. discuss the results of a large, multiinstitutional study of ^{18}F-DOPA PET scans of patients with Parkinson's disease, in an effort to provide centralized assessment of biomarkers of disease progression and therapy. . ***Page 1135***

Levivier et al. outline a technique that allows routine integration of functional PET data with stereotactic γ-knife neurosurgery in the treatment of brain tumors. . . . . ***Page 1146***

Simonian et al. report on a dual-isotope technique for simultaneous measurement of gastric emptying and accommodation in a single test that could prove beneficial for patients with upper gastrointestinal symptoms. . . . . ***Page 1155***

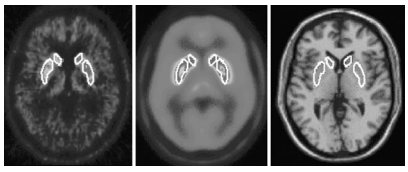

Becherer et al. compare ^{18}F-FDOPA PET and ^{111}In-labeled somatostatin receptor scintigraphy in imaging and staging of neuroendocrine tumors. . . . ***Page 1161***

de Jong et al. critique the assumption of homogeneous renal radioactivity in dose calculations for injected tracers and note the inadequacy of these assumptions for calculations in peptide receptor radionuclide therapy. . . . . ***Page 1168***

Kushner presents a continuing education review of clinical presentation, staging, prognosis, treatment, and nuclear medicine imaging options in neuroblastoma. . . . . ***Page 1172***

Tatsumi et al. report on the result of a study in rodents suggesting that drugs and environmental conditions can affect the high ^{18}F-FDG uptake of brown adipose tissue and suggest that such variables be considered routinely. . . . . ***Page 1189***

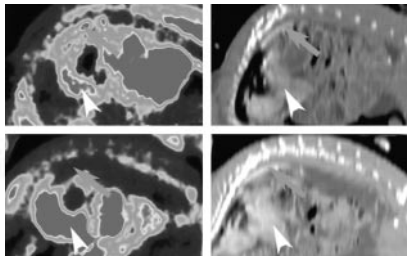

Sakuma et al. look at ^{99m}Tc labeling of myocardial microthromboemboli to provide both diagnostic and prognostic information on patients undergoing primary percutaneous transluminal coronary angioplasty. . . . . ***Page 1194***

Rusckowski et al. present evidence that ^{99m}Tc-labeled bacteriophages may exhibit specific binding to bacteria and bacterial fragments, suggesting the possibility of effective imaging for both diagnosis of infection and assessment of treatment. . . . . ***Page 1201***

Siaens et al. discuss the feasibility of and initial animal studies in SPECT of fungal infections with ^{123}I-labeled chitinase, a bacterium-derived enzyme. . ***Page 1209***

Rennen et al. investigate affinities to receptors on neutrophils and their suitability for infection imaging and suggest possible avenues for additional research. . . . . ***Page 1217***

Koppe et al. detail the characteristics of a range of radionuclides and their potential for use in radioimmunotherapy of small peritoneal metastases of colorectal origin. . . . . ***Page 1224***

Seltzer et al. provide new estimates for ^{11}C-acetate dosimetry in dynamic whole-body PET, suggesting that current recommended limits can be raised to improve overall image quality and tumor detection. . . . . ***Page 1233***

González Trotter et al. assess the feasibility of quantitative murine ^{124}I-antibody fragment PET using a large-bore clinical scanner that accommodates multiple animals simultaneously. . . . . ***Page 1237***

Ogawa et al. investigate the role of macrophages in ^{18}F-FDG accumulation in atherosclerotic lesions and the utility of PET in identifying vulnerable plaques. . . . . ***Page 1245***

Liu et al. present a novel technique using ^{99m}Tc-glucarate high-resolution SPECT for assessing the severity of myocardial injury induced by ischemia–reperfusion and point to possible applications in kinetic studies of new myocardial imaging agents. . . . . ***Page 1251***

Konijnenberg et al. present a computational rat model to facilitate and standardize organ dosimetry studies of peptide receptor radionuclide therapy and offer conclusions from initial calculations for ^{111}In, ^{117}Lu, and ^{90}Y. . . . . ***Page 1260***

ON THE COVER

The "motion-frozen" technique improves the display and quantification of gated myocardial perfusion SPECT images. Three-dimensional phase-to-phase motion vectors are derived by sampling the epi- and endocardial surfaces. In this illustration of displacement vectors used in image warping, the end-systolic epicardial surface is shown with perfusion data represented in color. Displacement vectors (white) show local motion between end systole and end diastole. The end-diastolic position of the epicardial surface is marked with red points.